

Selection effects shaping the Gamma Ray Burst redshift distributions

F. Fiore¹, D. Guetta¹, S. Piranomonte¹, V. D'Elia¹ and L.A. Antonelli¹

INAF — Osservatorio Astronomico di Roma, via Frascati 33, I-00040 Monteporzio Catone (Roma), Italy e-mail: fiore@oa-roma.inaf.it

March, 30 2007

ABSTRACT

Aims. Long Gamma Ray Bursts (GRBs) are associated to the death of massive stars and have been discovered, so far, up to $z=6.29$. Therefore, they hold the promise of probing star-formation and metal enrichment up to very high redshifts. However, the present GRB samples with redshift determinations are largely incomplete, and therefore a careful analysis of selection effects plaguing these samples is mandatory before any conclusion can be drawn from the observed GRB redshift distribution.

Methods. To this purpose we study and compare three well defined samples of long GRBs detected by Swift, HETE2 and BeppoSAX.

Results. We find that Swift GRBs are, on average, slightly fainter and harder than BeppoSAX and HETE2 GRBs, as expected due to the higher energy range (15-150 keV) in which Swift GRBs are detected and localized, compared to BeppoSAX and HETE2 ($\approx 2 - 20$ keV).

Gas and dust obscuration plays a role in shaping both the GRB samples and, most interestingly, the present samples of GRBs with redshift determination. In particular, we argue that the majority of the bright Swift GRBs without redshift might actually be $z \lesssim 2$ events, and therefore that the present Swift GRB sample with redshift is biased against low- z GRBs. On the other hand, the detection of bright UV rest-frame afterglows from high- z GRBs, and even from those with large X-ray obscuration, implies a dust amount lower than in nearby GRBs, and/or a different dust composition. If this is the case, the Swift sample of GRBs with redshifts is probably a fair sample of the real high- z GRB population. The absence of high- z GRBs in the BeppoSAX and HETE2 samples of GRBs with redshifts is probably due to the fact at the time of BeppoSAX and HETE2 follow-up faint afterglows of high redshift GRBs will have weakened below the spectroscopic capabilities of even 10m class telescopes.

The redshift distribution of a subsample of Swift GRBs with distributions of peak-fluxes, X-ray obscuration and optical magnitude at a fixed observing time similar to those of the BeppoSAX and HETE2 samples, is roughly consistent with the real BeppoSAX+HETE2 redshift distribution.

Key words. cosmology-observations; γ -ray sources; γ -ray bursts

1. Introduction

Gamma Ray Bursts (GRBs) are one of the great wonders of Universe. They combine several of the hottest topics of 21st century astrophysics. On one side they are privileged laboratories for fundamental physics, including relativistic physics, acceleration processes and radiation mechanisms. On the other side, being some GRBs associated to the death of massive stars (MacFadyen & Woosley 1999), it was soon realized after the discovery of their cosmologic origin, that they could be used as a cosmological tool to investigate star-formation and metal enrichment at the epochs of galaxy birth, formation and growth (e.g. Wijers et al. 1998, Porciani & Madau 2001, Fynbo et al. 2007). In this respect, two main research areas have developed. The first one uses GRBs as background beacons for spectroscopy of UV lines to characterize the physical and chemical state of the matter along the line of sight (Savaglio 2006 and references therein). The second includes statistical studies of the GRB redshift distributions (Guetta, Piran & Waxman 2005, Natarajan et al 2005, Jakobsson et al. 2006, Daigne et al. 2006). Even though the techniques adopted, and therefore the reference

communities, are somewhat different, these research areas are interconnected. As an example, UV lines can be used to determine the metal content of the absorption systems (D'Elia et al. 2006, D'Elia 2006b, Prochaska, Chen & Bloom 2006, Savaglio 2006). On the other hand, it is well known that galaxy-scale properties like metallicity, star-formation rate and mass are correlated. Then, metallicity determinations obtained through GRB spectroscopy can, at least in principle, be plugged in the GRB population studies, to obtain a better constraint on the models. In this paper we concentrate on population studies and in particular on the importance of selection effects in shaping GRB redshift distributions.

Population studies are very powerful tools. For example, galaxy and AGN counts and luminosity functions have been used to successfully measure the evolution of the star-formation rate, galaxy and black hole mass densities up to $z \lesssim 6$. Similarly, GRBs can be used to probe the histories of the GRB- and star- formation rates and of the metal enrichment in the Universe (e.g. Porciani & Madau 2001). Indeed, thanks to BeppoSAX first and then to HETE2 and Swift we begin having sizable samples of GRBs with reli-

able redshifts (about 80 up to now). This number should grow up to 150-200 within the Swift lifetime. This opens up the possibility to compute fairly well constrained GRB luminosity functions in a few redshift bins, and therefore measure the cosmic evolution of the GRB rate. The fraction of Swift GRBs with a reliable redshift is today about one third of the total. It might be expected that this fraction will improve in future, but it will hardly approach the majority of the GRBs. This means that the biggest problem we have to face in exploiting GRBs as cosmological tools is to understand and account for large selection effects. The role of large selection effects in shaping the population of GRBs with a measured redshift is evident when comparing the redshift distribution of Swift GRBs with that of BeppoSAX and HETE2 GRBs (figure 1). The median redshifts of the two distributions are 2.6 and 1.5 respectively. This discrepancy cannot be explained simply as due to the different detector sensitivity (e.g. Guetta & Piran 2007).

In the next sections we make a detailed description of what are the possible selection effects that plague the GRB redshift determination.

2. Samples used in this study

To gain more quantitative information on the issue of GRB selection effects we study three well defined sample of GRBs detected by Swift, HETE2 and BeppoSAX. We select long GRBs ($T_{90} > 3$ sec) outside the Galactic plane to limit Galactic extinction along their line of sight and to avoid too crowded fields, which can complicate the discovery of optical/NIR afterglows, and thus hamper redshift determinations. To this purpose we limit our study to regions with Galactic column density along the line of sight smaller than $\times 10^{21} \text{ cm}^{-2}$ (corresponding to $A_V \lesssim 1$). We also select GRBs with good (arcmin) localization. For BeppoSAX and HETE2 GRBs we require that the γ -ray burst is detected by the high energy GRBM and FREGATE instruments and is localized by the WFC, WXC or SXC instruments. For Swift we consider all long GRBs detected before September 10 2006, while for HETE2 we consider all long GRBs detected up to December 31 2003. For BeppoSAX we consider all GRBs detected during the entire mission. We excluded from the sample GRB 060218 and GRB980425, which are probably associated to a different class of events, orders of magnitude fainter than the rest of the sample (e.g. Guetta & Della Valle 2007). We consider only reliable spectroscopic redshifts. Table 1 gives more information on the selected samples.

Swift BAT peak-fluxes and spectral parameters are taken from the *Swift GRB Information page*¹.

Equivalent hydrogen column densities (N_H) are computed from X-ray afterglow spectra assuming solar abundances. Swift column densities are taken from (Campana et al. 2006) in 17 cases, from our own analysis in 12 cases and from the *Swift GRB Information page* in the rest of the cases. BeppoSAX peak-fluxes and spectral parameters, including hydrogen equivalent column densities, are taken from Stratta et al. (2004), Piro et al. (2005), and De Pasquale et al. (2006). For both samples the minimum column density is set to the Galactic value along the line of sight (Dickey & Lockman 1990). HETE2 peak-fluxes and spectral parameters are taken from Sakamoto et al. (2005).

Swift optical afterglow parameters are taken from the GCN through the *Gamma Ray Burst database*². BeppoSAX and HETE2 optical afterglow parameters are taken from the *Gamma Ray Burst database*, from Zeh et al. (2006) and from De Pasquale et al. (2006). Table 1 gives the number of optical afterglow detections and the number of cases in which multiple observations allowed us to estimate the optical afterglow decay index. We use wherever possible R band magnitudes. For 17 Swift GRBs and 1 BeppoSAX GRB we have only V band magnitudes, for 2 Swift GRBs only a white filter magnitude and for 8 BeppoSAX GRBs only g-band magnitudes. For all these GRBs we converted the observed magnitude into the R band using standard afterglow colors. The Lyman- α forest starts to enter the R band at $z=3.9$. Therefore, R band magnitudes for the GRBs at $z=4-5$ should be considered lower limits. For GRB050904 at $z=6.29$ we used TAROT I band equivalent magnitudes (Boer et al. 2006).

Table 1 gives also the number of reliable spectroscopic redshift obtained for the three samples. In most of the cases the redshift has been obtained through absorption lines overimposed on the afterglow spectrum. In a minority of cases (6, 3 and 2 for the Swift, BeppoSAX and HETE2 samples respectively) the redshift has been obtained uniquely through spectroscopy of the host galaxy, being the optical afterglow undetected or too faint to search for absorption features. In a few other cases the redshift has been obtained thanks to both absorption lines in the optical afterglow emission and host galaxy emission lines.

There are at least two large groups of selection effects that must be considered: (1) GRB detection and localization and (2) redshift determination through spectroscopy of the optical/NIR afterglow or of the GRB host galaxy. We discuss these two issues in the next sections.

3. GRB detection and localization

The sensitivity of BeppoSAX, HETE2 and Swift instruments as a function of the GRB spectral shape has been studied in detail by Band (2003, 2006). Band (2006) also studied the sensitivity of the BAT instrument as a function of the combined GRB temporal and spectral properties. We refer to these papers for more details on these topics.

Figure 2 compares the peak-flux cumulative distributions of the Swift GRBs with that of BeppoSAX and HETE2. The comparison is done in two energy bands: 15-150 keV, which is the band where BAT detects and localizes GRBs, and 2-26 keV, which is the band where the BeppoSAX WFC and the HETE2 WXC and SXC localize GRBs. To produce figure 2a) BeppoSAX GRBM and HETE2 Fregate peak-fluxes were converted to the 15-150 keV BAT band by using a power law model with an (average) energy index of 0.5 for the BeppoSAX bursts and the best fit model in Sakamoto et al. (2005) for the HETE2 bursts. To produce figure 2b) we used WFC and WXC peak-fluxes and converted BAT 15-150 keV peak fluxes in the 2-26 keV band by using the best fit models and parameters and the best fit observed column densities along the line of sight to the GRBs. To assess the robustness of our analysis we produced peak-flux cumulative distributions using different, but reasonable, values of the spectral parameters adopted for the conversion from one band to

¹ http://swift.gsfc.nasa.gov/docs/swift/archive/grb_table.html

² <http://grad40.as.utexas.edu/grblog.php>

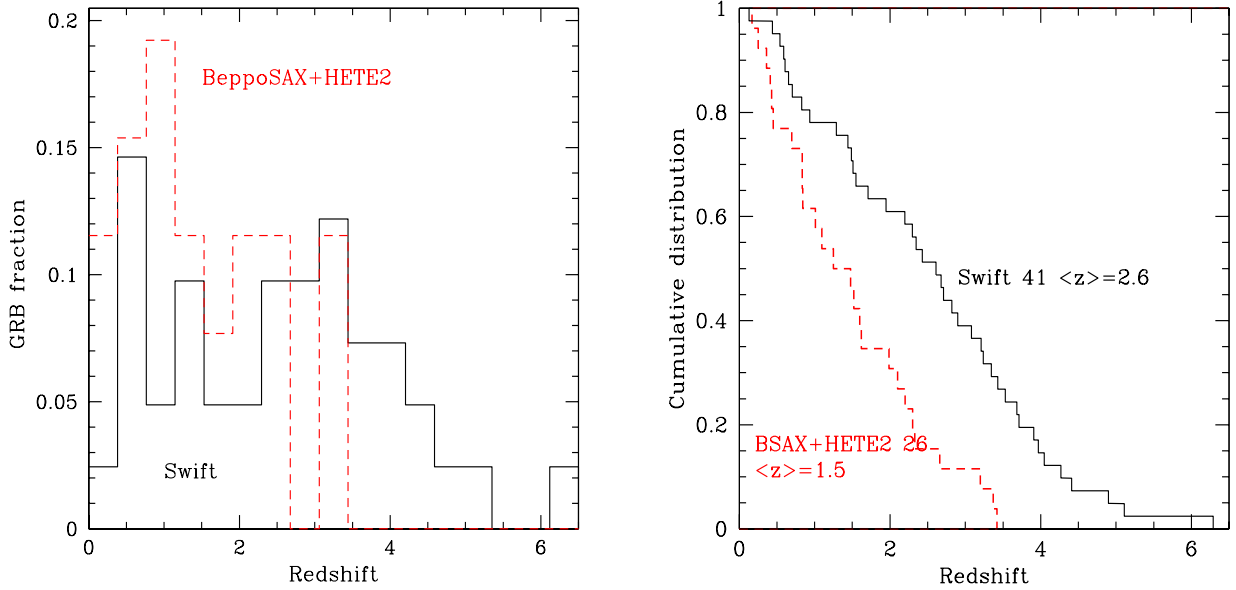


Fig. 1. Redshift distribution (left panel) and cumulative redshift distributions of Swift (solid line) and BeppoSAX+HETE2 (dashed line) GRBs.

Table 1. GRB samples

Sat.	Tot. GRB	O.A. ^a	O. decay ^b	Tot. z spec. ^c	z from em. lines ^d
Swift	122	62	44	41	6
BeppoSAX	39	18	16	12	3
HETE2	44	17	15	14	2

^a GRB with Optical Afterglows; ^b GRB with multiple optical observations and estimated optical afterglow temporal decay index; ^c total number of GRBs with a reliable spectroscopic redshift; ^d GRBs with a redshift derived only through spectroscopy of the host galaxy.

the other. We always found qualitatively similar results to those in figure 2.

Figure 2a) shows that Swift finds, on average, slightly fainter GRBs than BeppoSAX and HETE2 in the 15-150 keV band. The BeppoSAX and HETE2 samples contain a higher fraction of bright GRBs. The median $\log(\text{peak-flux})$ and its interquartile range are -6.93, 0.33 for the Swift sample and -6.88, 0.42 for the joined BeppoSAX+HETE2 sample. This is expected because of the better sensitivity of the BAT instrument with respect to the BeppoSAX GRBM and HETE2 Fregate instruments (Band 2003).

The median 2-26 keV $\log(\text{peak-flux})$ is -7.22, 0.32 for the Swift sample and -7.06, 0.38 for the joined BeppoSAX+HETE2 sample. The two 2-26 keV peak-flux distributions differ from each other more than the 15-150 keV distributions. This is probably due to the fact that Swift GRBs are localized at energies higher than 10-15 keV, while BeppoSAX and HETE2 GRBs are localized at energies $\lesssim 10$ keV. This implies that Swift localizes, on average, harder GRBs than BeppoSAX and HETE2. In particular, Swift GRBs are revealed in a spectral range in which absorption has little, if any, effect. A column density of $N_H = 10^{23} \text{ cm}^{-2}$ at $z=1$ would reduce the observed 2-10 keV flux by 12-15% (depending on the spectral index), thus reducing the probability of detecting such a highly obscured GRBs with BeppoSAX WFC and HETE2 WXC.

Conversely, these GRBs would certainly be present in the Swift sample.

Figure 3a) compares the best fit column density N_H in observer frame for the samples of Swift and BeppoSAX GRBs. The X-ray afterglows at the time of the BeppoSAX NFI observations (obtained repointing the satellite with a typical delay time of 8-10 hours from the GRB event), were significantly weaker than at the time of the Swift observations (typically minutes to a few hours after the GRB event), due to the afterglow power law decrease with exponent $\gamma = -1 : -2$. This implies that the uncertainties on the X-ray spectral parameters, and therefore N_H , are much bigger for BeppoSAX GRBs than for Swift GRBs. Indeed, the typical uncertainty of Swift column densities is $5 - 10 \times 10^{20} \text{ cm}^{-2}$ (see e.g. Campana et al. 2006), whereas that of BeppoSAX is ≈ 10 times larger (see Stratta et al. 2004 and De Pasquale et al. 2006). For this reason we plot 2 curves for the BeppoSAX GRBs. The leftmost curve assumes $N_H = N_H(\text{Galactic})$ for those GRBs whose best fit intrinsic N_H is consistent with zero. The rightmost curve is based on 90% upper limits on the N_H of these GRBs. The tail at high N_H values of this distribution is due to not well constrained upper limits. The real BeppoSAX N_H distribution is probably between the two curves.

Shortward of a few $\times 10^{21} \text{ cm}^{-2}$ the BeppoSAX curves in figure 3a) are significantly lower than the Swift curve. The probability that the BeppoSAX and Swift curves are

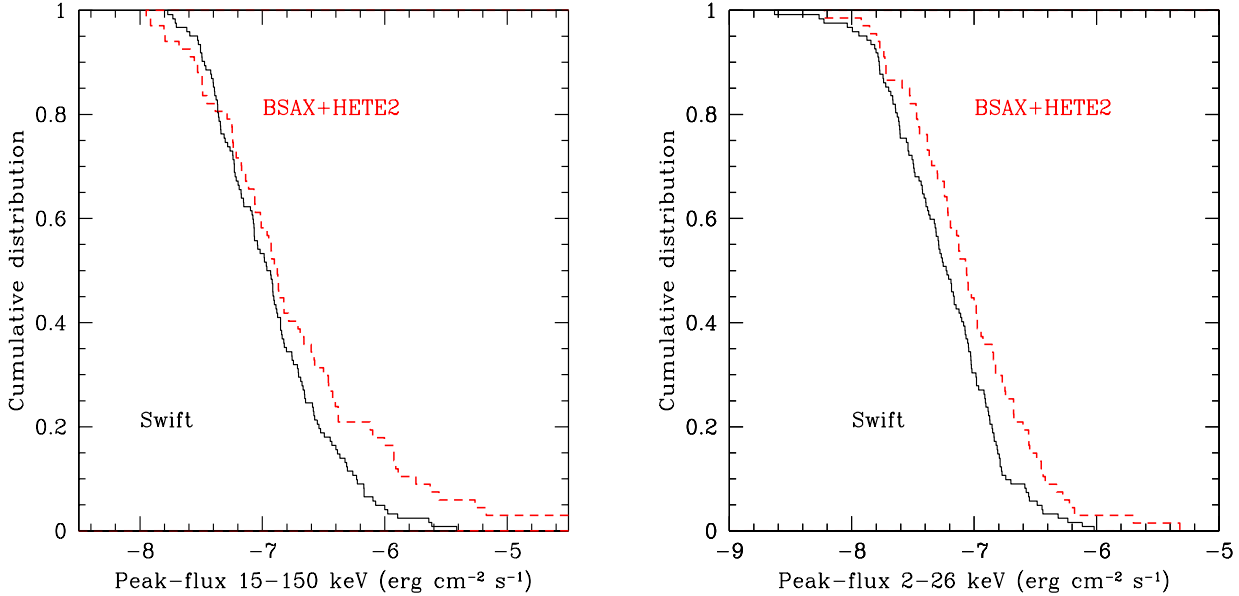


Fig. 2. Peak-flux cumulative distributions of the Swift (solid line) and BeppoSAX+HETE2 (dashed line) GRBs. a), left panel, 15-150 keV band; b), right panel, 2-26 keV band.

drawn from the same parent population is $< 10^{-5}$ and 1.7 % respectively, using the Kolmogorov-Smirnov test, thus confirming that Swift samples are less biased against obscuration than the BeppoSAX sample. Since the observer frame column density scales as the rest frame column density times $(1+z)$ to a large negative power (~ -2.5), this implies that the BeppoSAX sample is somewhat biased against low- z , highly obscured GRBs. Conversely, these GRBs must be present in the Swift sample.

Figure 3b) compares the N_H distribution of the Swift GRBs with determined redshift to that of the Swift GRBs with undetermined redshift. The probability that the two distributions are drawn from the same parent population is only 1%, suggesting that the sample of Swift GRBs with determined redshift is biased against GRB with large (observer frame) obscuration. Indeed, the N_H distributions of the Swift and BeppoSAX GRBs with redshifts are similar, unlike the N_H distributions of the full Swift and BeppoSAX GRBs, see above. This introduces the next important group of selection effects, those related to the determination of the redshift of a GRB through spectroscopy of the optical/NIR afterglow or of its host galaxy.

4. Redshift determination

In determining the redshift of a GRB the identification of the optical afterglow plays a major role. Only 6 Swift redshifts have been found through spectroscopy of the host galaxy (5 for the BeppoSAX and HETE2 joined sample).

Optical afterglows have been discovered for only 50% of the Swift GRB sample, a fraction only slightly greater than that of the BeppoSAX and HETE2 samples (46% and 39% respectively). This result is somewhat surprising, in consideration of the prompt Swift localization (minutes) and the large international effort on Swift GRB follow-up observations, which exploits an impressive number of facilities, from dedicated robotic telescopes to 8m class telescopes

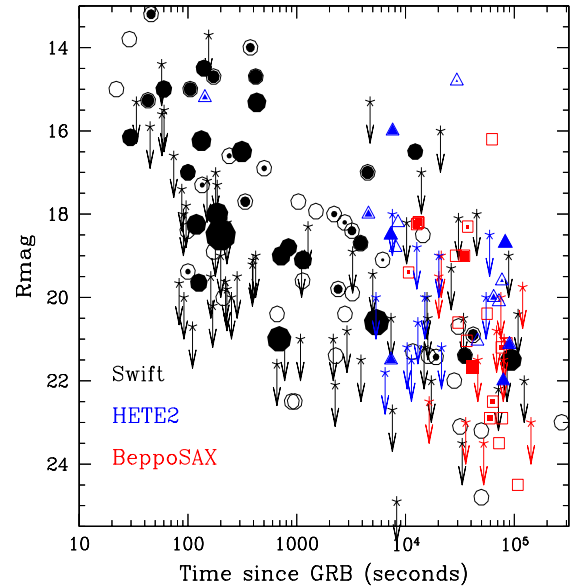


Fig. 4. The R magnitude of the optical afterglow at the time of its discovery as a function of this time. Filled symbols are GRBs with reliable redshift determination. The size of the symbol is proportional to the redshift (the larger the symbol the larger the redshift). Circles = Swift GRBs; squares = BeppoSAX GRBs; triangles = HETE2 GRBs.

like the VLT, Gemini and Keck. It was expected that such an effort would have produced a much larger fraction of optical/NIR afterglow identifications than BeppoSAX and HETE2.

Figure 4 shows the R magnitude of the optical afterglow as a function of the time of discovery of the optical afterglow the Swift, BeppoSAX and HETE2 GRBs. As ex-

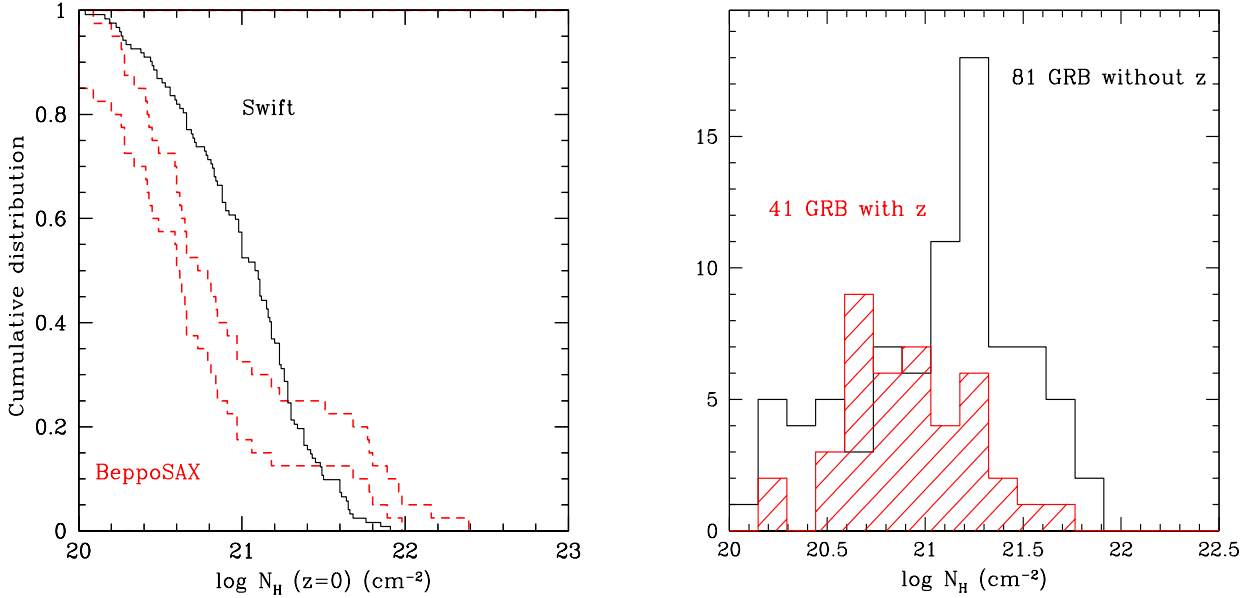


Fig. 3. a), left panel, N_H cumulative distributions of the Swift (solid line) and BeppoSAX (dashed lines) GRBs. The leftmost BeppoSAX curve assumes $N_H = N_{H, \text{Galactic}}$ for the GRBs with a best fit intrinsic N_H consistent with zero. The rightmost BeppoSAX curve assumes for these GRBs the 90% upper limit. b), right panel, N_H histograms of the Swift GRB with (shadow histogram) and without redshift (black histogram).

pected, redshifts are preferentially found for bright afterglows. The figure suggests also that at a given time from the GRB event the Swift optical afterglows are fainter, on average, than the BeppoSAX and HETE2 afterglows. We then computed the magnitude of the Swift, BeppoSAX and HETE2 afterglows at a fixed time using the best fit decay indices found for each GRB afterglow, when available. In the rest of the cases we used a time decay index of -1. We chose a fixed time of 10ks after the burst (observer frame), which is intermediate between the typical times at which Swift, BeppoSAX and HETE2 GRBs are discovered, thus minimizing the extrapolation to compute the R mag at 10ks.

Figure 5a) compares the Swift distribution of the R mag at 10 ks from the GRB event with that of the BeppoSAX and HETE2. GRBs without detection of optical afterglow but for which optical follow-up observations were carried out are included in this distribution at the magnitude of their upper limits. This figure confirms that Swift finds bursts with a fainter optical afterglow. The probability that the Swift and BeppoSAX+HETE2 distributions are drawn from the same parent population is $< 10^{-5}$. Similar results are obtained by considering the distributions of the magnitudes of the detected afterglows, excluding the upper limits. In principle, the fainter Swift optical afterglows may be due to the fact that Swift detects, on average, fainter GRBs (see figure 2). However, this is probably not the case. Figure 5b) shows the Swift and BeppoSAX+HETE2 distributions of the γ -ray (15-150 keV) to optical (R band) flux ratio. (Also in this case GRBs with undetected optical afterglow are included at the magnitude of their upper limits.) The probability that the two distributions are drawn from the same parent population is smaller than 1%. This probability increases to 1.6% by comparing the distributions of the magnitudes of the detected afterglows, excluding the upper

limits. Similar results are obtained considering the X-ray (2-26 keV) to optical flux ratio. Computing the R magnitude at 1 ks or at 100 ks does not change qualitatively this result.

5. Selection effects at work

There two major differences in the Swift and BeppoSAX+HETE2 redshift distribution: a) a relatively large number of GRB with $z > 3.5$ is present in the Swift sample (11 out 41 GRB, i.e. 27 % of the sample). These GRBs are absent in the combined BeppoSAX+HETE2 sample. b) a deficit of low redshift ($z \lesssim 2$) in the Swift sample with respect to what would be expected based on the BeppoSAX+HETE2 sample. We discuss these two points in turn.

About the first point, the Swift better sensitivity to faint GRBs and the Swift quick localization may explain the presence of a large number of high redshift GRBs in the Swift sample compared to the BeppoSAX and HETE2 samples. First, the highest redshift GRBs are found at low peak-fluxes in figure 6a), which plots the redshift as a function of the 15-150 keV peakflux for the Swift, BeppoSAX, and HETE2 GRB samples. Second, the Swift capability to localize the GRB on time-scales of minutes allows the discovery of faint optical afterglows, that can be promptly observed in spectroscopic mode. The median delay time of optical follow-up for the Swift, HETE2 and BeppoSAX GRBs is 15 minutes, 3.5 hours and 14 hours respectively. If optical and near infrared afterglows decreases like power laws with exponent $\gamma \approx -1$, they would have faded by 2.9 and 4.4 magnitudes passing from the median Swift delay time to the median HETE2 and BeppoSAX delay times, respectively. Faint afterglows of high redshift GRBs will have weakened even below the spectroscopic capability of 10m

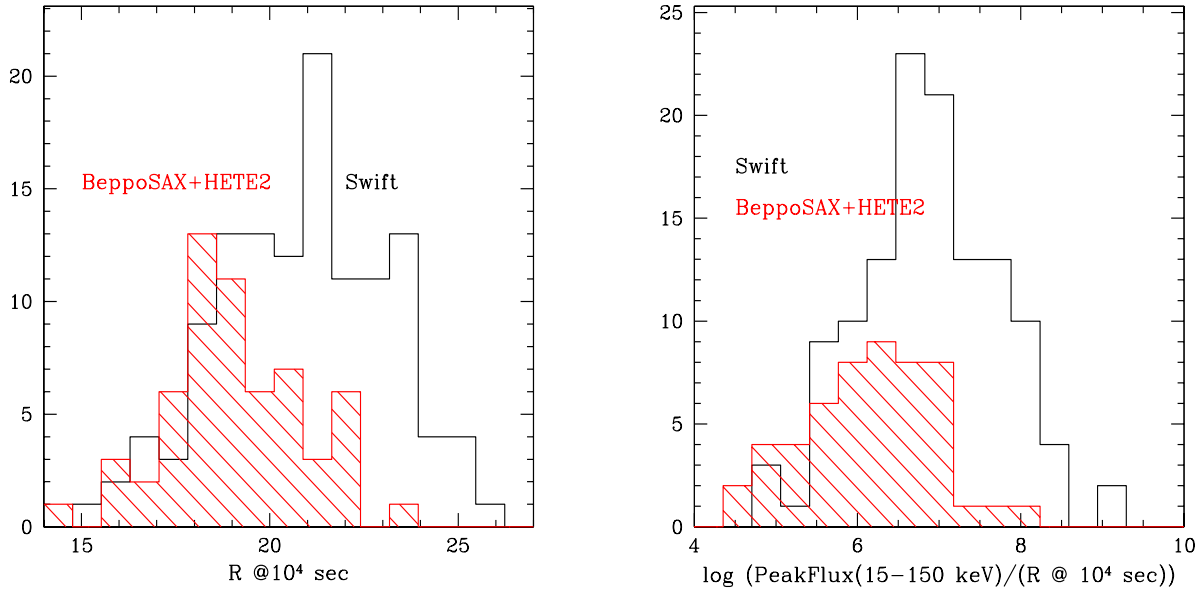


Fig. 5. a), left panel, the distribution of the R magnitude 10ks after the GRB events for the Swift (solid histogram) and the BeppoSAX+HETE2 (dashed histogram) GRB samples. GRBs without detection of optical afterglow but for which optical follow-up observations were carried out are included in this distribution at the magnitude of the corresponding upper limits. b), right panel, the distribution of the γ -ray (15-150 keV) to optical (R band) flux ratio for the Swift (solid histogram), and BeppoSAX+HETE2 (red histogram) GRB samples.

class telescopes, if observed many hours later like in the BeppoSAX and HETE2 era. Furthermore, the host galaxies of high redshift GRBs are too faint to allow redshift determinations through their emission lines.

The discrepancy between the Swift and BeppoSAX+HETE2 samples at low redshift is less straightforward and requires a more detailed discussion. Figure 6a) shows that the peak-flux distribution becomes wider at low redshift. Indeed, the median redshift of the 24 Swift GRB with 15-150 keV peak-flux $> 3 \times 10^{-7}$ erg cm $^{-2}$ ($\sim 20\%$ of the sample) is only $\langle z \rangle = 1.5$, very different from the median redshift of the full sample ($\langle z \rangle = 2.6$). The sample of bright GRBs is particularly useful because: a) selection effects due to temporal and spatial variation of the instrument sensitivity are minimized; and b) the redshift range is narrower, being high- z GRBs systematically fainter than bright GRBs, thus minimizing evolutionary effects. For bright fluxes the sensitivity of the instruments can be safely considered constant over their entire field of view, and it is therefore easier to compare the number of GRBs expected by different experiments. Comparing the field of view of Swift BAT to that of the BeppoSAX WFC, and considering the net observing time spent by the two satellites searching for GRBs, we expect a number of bright GRBs (15-150 keV peak-flux $> 3 \times 10^{-7}$ erg cm $^{-2}$) ~ 1.5 times higher in the Swift sample than in the BeppoSAX sample, a factor similar to that found in the real GRB samples (1.77). Conversely, the number of bright GRBs with $z < 2$ in the Swift sample is only half that in the BeppoSAX sample (4 against 8). It is clear that a strong selection effect is at work, biasing the sample of Swift GRBs with redshift against low- z sources. Indeed, only 7 out of 24 bright Swift GRBs have a spectroscopic redshift, to

be compared to 8 out of 13 in the BeppoSAX sample (and 3 out of 6 of the HETE2 sample).

A possible cause of the difficulty in obtaining a redshift for many bright Swift GRBs is obscuration. The median observer-frame column density toward the bright Swift GRBs is $\log N_H = 21.28$ with an interquartile range of 0.24, while the median $\log N_H$ of the faint Swift GRBs is $\log N_H = 21.0$ with interquartile 0.30. The probability that the two $\log N_H$ distribution are drawn from the same parent population is $\lesssim 2\%$. The median $\log N_H$ of the 13 BeppoSAX GRBs with 15-150 keV peak-flux $> 3 \times 10^{-7}$ erg cm $^{-2}$ is 20.66 (or 20.97 assuming the 90% upper limit for the GRBs with a best fit intrinsic N_H consistent with zero). The intrinsic observer-frame $\log N_H$ (i.e. after subtraction of the Galactic column density along the line of sight) of the 24 Swift bright GRBs is 21.10. At a typical redshift of 1.5 this implies a rest-frame column density of $\log N_H \sim 22.1$ and an optical extinction of several magnitudes, assuming a Galactic dust to gas ratio. This dust extinction would make more difficult both the discovery of optical afterglows and the determination of the redshift through optical spectroscopy. Indeed, the fraction of detected optical afterglows among the bright Swift GRBs is 46%, slightly smaller than that of the sample of the 98 Swift GRBs with 15-150 keV peak-flux $< 3 \times 10^{-7}$ erg cm $^{-2}$ (52 %). The median R band magnitudes of the bright GRBs ($\langle R \rangle = 18.4$) is also similar to that of the faint GRBs ($\langle R \rangle = 18.7$). Nearly identical are the median R magnitudes at 10 ks, $\langle R \rangle = 20.73$ for bright GRBs and $\langle R \rangle = 20.72$ for the faint GRBs. Conversely, one would expect fainter optical afterglows for the fainter GRBs. Finally, the fraction of bright Swift GRB with redshift is only 29% while that of bright BeppoSAX and HETE2 GRBs is 62 % and 50 % respectively, despite the much quicker optical follow-

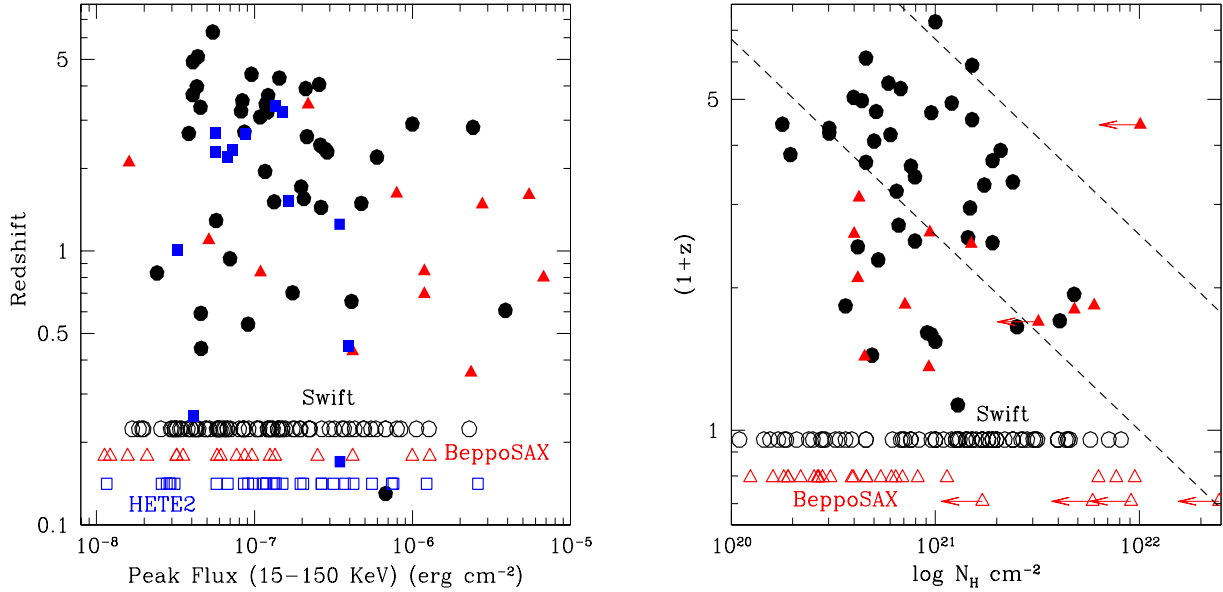


Fig. 6. The redshift as a function of the 15-150 keV peak-flux (a), left panel) and of the observer frame N_H (b), right panel) for the Swift (cycles), BeppoSAX (triangles) and HETE2 (squares) GRBs. GRB without a measured redshift are plotted at a constant z as empty symbols. The left dashed line in figure 6b) is the expectation for a constant, rest-frame column density of $\log N_H = 22$, the right dashed line is the expectation for $\log N_H = 23$.

up observations for Swift GRBs. Excluding the objects with redshift obtained from host galaxy emission lines from these samples does not change this conclusion.

Figure 6b) plots the redshift as a function of the observer frame N_H for the Swift and BeppoSAX GRB samples. Not surprisingly the highest redshift GRBs are found not only at low peak-fluxes (figure 6a), but also at low observed column densities. The two dashed lines in figure 6b) are the expectation for a constant, rest-frame column density of $\log N_H = 22$ (left line) and $\log N_H = 23$ (right line). The observed Swift $\log N_H$ distribution is consistent with the expectation of rest frame column densities of the order of 10^{22} cm^{-2} , typical of dense molecular clouds. GRBs with rest-frame obscuring column densities of the order of 10^{23} cm^{-2} do exist. Such high column densities have been detected only in high z GRBs so far (GRB050904 at $z=6.29$ and GRB060510B at $z=4.9$). These column densities imply a huge extinction of the rest-frame UV light, if dust with properties similar to that in the Galaxy, the SMC or even for a dust with a grain distribution strongly shifted toward large grain sizes (Stratta et al. 2004, 2005) would be associated to the X-ray absorbing gas. The simple detection of the bright optical and near infrared afterglow of this GRB (Tagliaferri et al. 2005, Haislip et al. 2006, Boer et al. 2006) implies peculiar dust properties (Campana et al. 2006b, Stratta et al. 2007). Here we limit ourselves to note that high- z GRBs with a gas column density similar to that of GRB050904 but with less extreme dust properties would easily remain undetected in the optical and near infrared. Furthermore, their host galaxies would be so faint that unambiguous associations with the GRB would be impossible, because the probability to find such faint galaxies in the arcsec Swift XRT error-boxes would be not negligible, thus making impossible the determination of their redshift.

To assess more quantitatively how the different selection effects (peak-flux limit, GRB obscuration and magnitude of the optical afterglow) can modify the redshift distribution we extracted from the Swift GRB sample a subsample having the same peak-flux, N_H and $R_{\text{mag}}(\text{at } 10\text{ks})$ distributions of the joined BeppoSAX+HETE2 sample (the “constrained” GRB sample hereafter). Figure 7 compares the redshift distribution of the constrained GRB sample with that of the full Swift and BeppoSAX+HETE2 GRB samples. To evaluate the uncertainty on the constrained GRB sample redshift distribution we ran the random extraction 100 times and plot the contours of the region covered by the constrained GRB sample redshift distributions. We see that the constrained GRB sample redshift distribution is consistent, to within the uncertainties, with the real BeppoSAX+HETE2 redshift distribution.

Other, more subtle, selection effects may be at work as well. For example, there are redshift ranges for which the typical interval covered by optical spectrometers ($\approx 3800\text{--}8000 \text{ \AA}$) does not contain any strong emission or absorption line. For example, strong emission lines such as $H\alpha$, $H\beta$, $[OIII]\lambda\lambda 4959, 5007$, $[OII]\lambda 3725$ go out of the above wavelength range at $z \sim 1.1$, while Lyman- α enter the range at $z \sim 2.1$. The redshift range 1.1-2.1 is the so called “redshift desert”. Analogously, the strongest absorption feature, after Lyman- α is the $\text{MgII}\lambda\lambda 2796, 2803$ doublet. This goes in a region strongly affected by telluric features already at $z \gtrsim 1.5$. So redshift determinations through absorption lines in low signal to noise spectra are difficult in the redshift range 1.5-2.1. In any case, treating quantitatively these effects is difficult, because of the very diverse quality of the optical spectra of GRB afterglows. Unfortunately, because of the highly variable nature of these events, afterglow observations have often performed

in non-optimal conditions and instrument set-ups, and most importantly, they cannot be repeated.

6. Conclusions

We have compared three well defined samples of long GRBs observed and localized by Swift (122 GRBs), BeppoSAX (39 GRBs) and HETE2 (44 GRBs), for a total of 205 objects. Secure spectroscopic redshifts have been measured for 67 of these GRBs. The fraction of redshift determinations is similar in the three samples, 34 %, 30% and 32% respectively.

Swift GRBs are, on average, slightly fainter and harder than BeppoSAX and HETE2 GRBs. This is probably due to both the better sensitivity of the BAT detector with respect to the BeppoSAX and HETE2 detectors and to the higher energy range (15-150 keV) where Swift GRBs are detected and localized, compared to BeppoSAX and HETE2 ($\approx 2 - 20$ keV). The distribution of the observer frame N_H for the Swift GRBs is shifted toward higher N_H values than BeppoSAX, at a confidence level of better than 98%. This is again probably due to the different energy bands in which GRBs are localized by the two satellites. The most obscured GRBs have probably been missed by the BeppoSAX survey. The distribution of the observer frame N_H for the Swift GRBs without redshift determination is also shifted toward higher N_H values than that of the Swift GRBs with a redshift determination (confidence level of better than 99%), implying that the sample of Swift GRBs with redshift determinations is biased against large obscuration. This is confirmed by a more detailed analysis of the sample of bright GRBs. If dust is associated to the X-ray absorbing gas, one would expect that extinction makes the discovery and study of optical afterglows of bright Swift GRBs more difficult. This is probably the case, since the fraction of bright Swift GRB with redshift is only 29% while that of bright BeppoSAX and HETE2 GRBs is 62 % and 50 % respectively. Highly obscured, bright, low redshift GRBs are likely present in the Swift sample, but so far most of them must have escaped redshift determination (we expect that the majority of the 17 bright Swift GRBs without redshift are at $z \lesssim 2$). A program to discover and measure the magnitude and the redshift of the host galaxies of bright Swift GRBs could confirm this conclusion and provide a sample of GRB redshifts unbiased against obscuration.

Highly X-ray obscured GRBs do exist also at high redshift. The detection of bright optical and near infrared (UV rest frame) afterglows from these GRBs implies a dust to gas ratio and/or dust composition different from those of nearby GRBs (Stratta et al. 2007). Indeed, at $z \gtrsim 5$ the major source of dust in the local Universe (AGB stars) falls short of time to produce enough dust, implying that high- z GRB host galaxies probably contains much less dust than lower redshift host galaxies. This implies that redshift determination of high- z GRBs would not be more difficult than that of lower redshift GRBs, even if the observed optical and near infrared bands sample the UV rest frame. If this is the case, the Swift sample of GRBs with redshifts would be a fair sample of the real high- z GRB population.

The absence of high redshift GRBs in the BeppoSAX and HETE2 samples of GRBs with measured redshift is most likely due to the fact that the median delay between the GRB event and the optical and near infrared follow-ups for BeppoSAX and HETE2 GRBs is ~ 50 times and

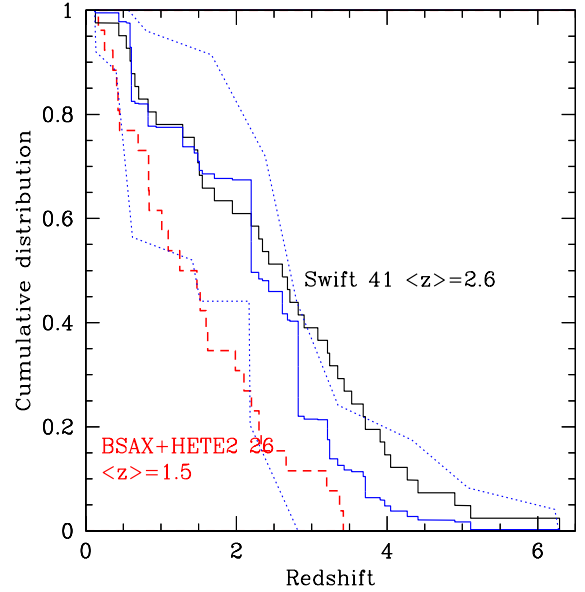


Fig. 7. The average cumulative redshift distribution of a subsample of Swift GRBs having the same peak-flux, N_H and $R_{\text{mag}}(\text{at } 10\text{ks})$ distributions of the joined BeppoSAX+HETE2 samples (thin solid line) compared with the Swift (thick solid line) and BeppoSAX+HETE2 (dashed line) total redshift distributions. The thin dotted lines mark the redshift range covered by 100 random extractions and give an idea of the statistical uncertainty associated to a single extraction of a redshift distribution of 26 GRBs from a parent population.

~ 15 times longer than that of Swift GRBs. At the time of BeppoSAX and HETE2 follow-up faint afterglow of high redshift GRBs are too faint to allow redshift determination through absorption line spectroscopy. Furthermore, the host galaxies of high redshift GRBs are too faint to allow redshift determination through their emission lines. High redshift GRBs may well be present in the BeppoSAX and HETE2 samples, but it is extremely difficult, if not impossible, to determine their redshift and therefore recognize them as such.

Swift optical afterglows, measured at a fixed observer frame time, e.g. 10 ks after the GRB event, are fainter than BeppoSAX and HETE2 optical afterglows, also when compared to the GRB 15-150 keV peak-flux. This is somewhat surprising, because the higher median redshift of Swift GRBs implies that a fixed observer-frame time samples, on average, a shorter rest-frame time delay from the GRB event for the Swift GRBs than BeppoSAX and HETE2. Because afterglows decrease like power laws one would expect that the ratio between the GRB peak-flux and the optical afterglow magnitude at a fixed observed time would be smaller for the Swift afterglows, contrary to what is observed. At least two effects may contribute to explain the observed trend. The first is that at $z > 4$ the Lyman- α forest enters the R band, thus reducing the observed optical flux. The second is a higher extinction in Swift GRBs with respect to BeppoSAX and HETE2 GRBs, as discussed above.

To conclude at least selection effects on GRB localization and GRB redshift determination must be properly

taken into account in order to safely use GRBs as cosmological tools, and derive the physical and cosmological evolution of the GRB formation rate from statistical analysis of the present GRB samples, at least selection effects on GRB detection. This would allow a fair and quantitatively-meaningful comparison with the star-formation rate estimated through other means. Moreover, star-formation in regions hardly reachable by other techniques (low mass, dwarf galaxies, high redshift galaxies, dust enshrouded star-formation sites) could be probed.

Acknowledgments We thank Rosalba Perna and Elena Rossi for early discussions on the topics presented in this papers. We also thank Eli Waxman for useful comments and Luigi Stella for a careful reading of the manuscript. We acknowledge support from contracts ASI/I/R/039/04 and ASI/I/R/023/05/0.

References

- Band, D.L. 2003 ApJ, 588, 945
 Band, D.L. 2006 ApJ, 644, 378
 Boer, M., Atteia, J.L., Damerdj, Y., Koltz, A., & Stratta, G. 2006, ApJL, 638, L71
 Campana, S, Romano, P., Covino, S. et al., 2006, A&A, 449, 61
 Campana, S., Lazzati, D., Ripamonti, E., et al. 2006, ApJL in press, astro-ph/0611305
 Daigne, F., Rossi, E.M. & Mochkovitch, R. 2006, MNRAS, 372, 1034
 D'Elia, V., Fiore, F., Piranomonte, S. et al. 2006, A&A, in press, astro-ph/0609825
 D'Elia, V., Piranomonte, S., Ward, P., Fiore, F., Meurs, E.J.A., & Norci, L. 2006, proceedings of the meeting *The Multicoloured Landscape of Compact Objects and their Explosive Origins*, AIP, Burderi L. et al. ed., in press.
 De Pasquale, M., Piro, L., Gendre, B. et al. 2006, A&A, 455, 813
 Dickey J.M. & Lockman F.J. 1990, ARA&A, 28, 215
 Fynbo, J.P.U., Hjorth J., Malesani, D., Sollerman, J., Watson, D., Jakobsson, P., Gorosabel, J., Jaunsen, A.O. 2007, proceedings of the Eleventh Marcel Grossmann Meeting on General Relativity, eds. H. Kleinert, R. T. Jantzen & R. Ruffini, astro-ph/0703458
 Guetta, D., Piran, T. & Waxman, E. 2005 ApJ, 619, 412
 Guetta, D. & Piran, T. 2007, A&A submitted, astro-ph/0701194
 Guetta, D. & Della Valle, M. 2007, ApJL in press, astro-ph/0612194
 Jakobsson, P., Levan, A., Fynbo, J.P.U. et al. 2006, A&A, 447, 897
 Haislip, J.B., Nysewander, M.C., Reichart, D.E. et al. 2006, Nature, 440, 181
 Lockman, F.J. & Condon, J.J. 2005, AJ, 129, 1968
 MacFadyen, A. I. & Woosley, S. E., 1999, ApJ, 524, 262
 Natarajan, P., Albanna, B., Hjorth, J., Ramirez-Ruiz, E., Tanvir, N. & Wijers, R. 2005, MNRAS, 364, L8
 Piro, L., De Pasquale, M., Soffitta, P. et al. 2005 ApJ, 623, 314
 Porciani, C. & Madau, P. 2001, ApJ, 548, 522
 Prochaska, J. X., Chen, H. & Bloom, J. 2006, ApJ, 648, L97
 Sakamoto, T., Lamb, D.Q., Kawai, N. et al. 2005 ApJ, 629, 311
 Savaglio, S. 2006, New journal of Physics, 8, 295, astro-ph/0609489
 Stratta, G., Fiore, F., Antonelli, L.A., Piro, L., De Pasquale, M. 2004, ApJ, 608, 846
 Stratta, G., Perna, R., Lazzati, D., Fiore, F., Antonelli, L.A., Conciatore, M.L. 2005, A&A, 441, 83
 Stratta, G., Maiolino, R., Fiore, F., D'Elia, V. 2007, ApJL in press, astro-ph/0703349
 Tagliaferri, G., Antonelli, L.A., Chincarini, G., et al. 2005, A&A, 443, L1
 Wijers, R.A.M.J. et al. 1998, MNRAS, 294, L13
 Zeh, A., Klose, S. & Kann, D.A. 2006, ApJ, 637, 889

